Full Paper

Direct Electrochemistry of Hemoglobin Immobilized on Colloidal Gold-Hydroxyapatite Nanocomposite for Electrocatalytic Detection of Hydrogen Peroxide

Juan You[a,b] *Weiping Ding*,[b] *Shijia Ding*,[a]* *Huangxian Ju*[a,b]*

[a] Key Laboratory of Medical Diagnostics (Ministry of Education of China), Department of Laboratory Medicine, Chongqing Medical University, Chongqing 400016, P. R. China
[b] Key Laboratory of Analytical Chemistry for Life Science (Ministry of Education of China), Department of Chemistry, Nanjing University, Nanjing 210093, P. R. China
*e-mail: hxju@nju.edu.cn

Received: September 1, 2008
Accepted: November 14, 2008

Abstract
A novel nanocomposite of colloidal gold (GNPs) and hydroxyapatite nanotubes (Hap) was prepared for immobilization of a redox protein, hemoglobin (Hb), on glassy carbon electrode. The immobilized Hb showed fast direct electron transfer and excellent electrocatalytic behavior toward reduction of hydrogen peroxide. A synergic effect between GNPs and Hap for accelerating the surface electron transfer of Hb was observed, which led to a pair of redox peaks with a formal potential of (-340 ± 2) mV at pH 7.0, and a new biosensor for hydrogen peroxide with a linear range from 0.5 to 25 μM and a limit of detection of 0.2 μM at 3σ. Owing to the good biocompatibility of the nanocomposite, the biosensor exhibited good stability and acceptable reproducibility. The as-prepared nanocomposite film provided a good matrix for protein immobilization and biosensor preparation.

Keywords: Hydroxyapatite, Gold nanoparticles, Nanocomposite, Hemoglobin, Direct electrochemisty, Biosensor

DOI: 10.1002/elan.200804446

1. Introduction

The direct electrochemistry of redox proteins can establish a desirable model for fundamental study of electron transfer chain in biological systems. Meanwhile, the direct electron exchange between proteins and underlying electrodes can provide a platform for fabrication of biosensors, enzymatic bioreactors, and biomedical devices [1–6]. Hemoglobin (Hb), an important redox protein, functions physiologically in the storage and transport of molecular oxygen in the blood of vertebrates, comprised of four polypeptide subunits (two α- and two β-polypeptide chains), each of which has an iron-bearing heme within molecular accessible crevices and has a similar structure. Although Hb does not play a role as an electron transfer carrier in biological systems, it has been shown to possess enzyme-like catalytic activity [7, 8]. Thus it is generally used as an ideal molecule for the study of electron transfer reactions of heme proteins because of its commercial availability, moderate cost, and its known and documented structure besides its intrinsic peroxidase activity. However, the electron transfer between Hb and the supporting metal substrate is very slow mainly due to the fact that the electroactive centers of Hb are deeply buried in the polypeptide and inaccessible to the surface of electrodes [9, 10]. The modification of electrode surfaces with different materials such as surfactants [11, 12], polymer [13, 14] and nanoparticles [15, 16] has been performed for accelerating the surface electron transfer of Hb. This work prepares a novel nanocomposite of colloidal gold nanoparticles (GNPs) and hydroxyapatite (Hap) nanotubes to immobilize Hb on a glassy carbon electrode. The GNPs-Hap nanocomposite can greatly accelerate the direct electron transfer.

Hap ($Ca_{10}(PO_4)_6$), a bioceramic analogous to the mineral component of bone with good biocompatibility and particular multi-adsorbing sites, has attracted a lot of attention because of its extensive applications such as tooth implants [17], adsorbents [18, 19] and protein separation [20, 21]. Owing to the high surface area and strong adsorption ability of Hap nanostructure, a film of hydroxyapatite-chitosan nanoparticles has been electrodeposited on an electrode surface for construction of label-free capacitive immunosensor for human transferrin [22]. A piezoelectric immunosensor for α-fetoprotein has also been fabricated by immersing a crystal in a suspension of GNPs/Hap particles and then an α-fetoprotein antibody solution [23]. The particles were prepared by dispersing nanosized Hap in Au colloid solution and then drying the resulting hybrid materials.

GNPs have been extensively used to study the direct electrochemistry of proteins such as cytochrome c [24], horseradish peroxidase [25], glucose oxidase [26] and hemoglobin [15, 27–29, 30–33]. They can provide an environment similar to that of redox protein in a native

system and allow the protein molecules more freedom in orientation, thus reducing the insulating property of protein shells for direct electron transfer and facilitating the electron transfer though the conducting tunnels of colloidal gold [5]. However, owing to the poor film-forming of GNPs, it is necessary to provide a matrix to produce GNPs film. This work uses Hap nanotubes as the support for convenient formation of film containing GNPs. Different from the Hap particles in [22, 23], the tube-typed nanostructure is favorable to the formation of homogeneous nanocomposite. Furthermore, upon the immobilization of Hb the resulting GNPs-Hap nanocomposite coating shows a synergistic effect between GNPs and Hap nanotubes for accelerating the surface electron transfer of Hb, and the electrocatalytic activity toward reduction of hydrogen peroxide, leading to a biosensor with excellent performance due to the high surface area and satisfactory biocompatibility of the new nanocomposite.

2. Experimental

2.1. Materials and Reagents

Hemoglobin (from bovine blood) was obtained from Sigma and used without further purification. 10 mg mL^{-1} of Hb solution was stored at 4 °C as stock solution. $HAuCl_4 \cdot 3H_2O$ was purchased from Aldrich (Deisenhofen, Germany). H_2O_2 (30% w/v solution) was purchased from Shanghai Chemical Reagent Co. (China). 0.1 M phosphate buffer solutions (PBS) with various pH values were prepared by mixing the stock standard solutions of Na_2HPO_4 and NaH_2PO_4. All other chemicals were of analytical reagent grade and used as received, doubly distilled water was used throughout.

2.2. Apparatus and Measurements

Electrochemical measurements were carried out with a CHI 660A electrochemistry workstation (Shanghai CH Instruments, China). A standard three-electrode system, which comprised of a modified electrode as working, a platinum wire as auxiliary and a saturated calomel electrode (SCE) as reference electrodes, was used for all electrochemical experiments. The cyclic voltammetric (CV) and amperometric measurements were performed in an electrochemical cell containing 10 mL of 0.1 M PBS (pH 7.0) at room temperature, which was deoxygenated by bubbling highly pure nitrogen for 20 min and kept in nitrogen atmosphere during measurements. UV-vis absorbance spectra were recorded using a UV-vis-3600-Nir Recording Spectrophotometer (Shimadzu, Japan). The scanning electron micrographs were taken with scanning electron microscope (SEM, S-4800, Hitachi).

2.3. Preparation of Biosensor

2.3.1. Preparation of GNPs-Hap Nanocomposite

The Hap nanotubes were prepared by a chemical precipitation and hydrothermal technique according to the modified literature procedure [34]. In brief, an aqueous solution of H_3PO_4 (0.3 M, 300 mL) was added dropwise to vigorously stirred aqueous solution of $Ca(OH)_2$ (0.25 M, 625 mL) at a rate of 1 mL min^{-1} at 60 °C, and the pH of the resulting suspension was adjusted to pH 7.0. After aging, the HAP nanotubes could be formed and purified by repeated washing with distilled water and centrifugation at 2500 rpm for 20 min (5 ×).

GNPs with 24-nm diameter were prepared by adding 0.5 mL of 1% Na_3-citrate solution to a boiling 50 mL solution of 0.01% $HAuCl_4$ and maintaining the mixture at the boiling point for 15 min and stirred for another 15 min [27, 35]. The preparation was stored in a brown glass bottle at 4 °C.

The GNPs-Hap nanocomposite could be obtained by mixing a suspension of 0.2 mg mL^{-1} Hap nanotubes and the as-prepared Au colloid solution with sonication for about 10 min. The optimal ratio of the suspension to colloid solution was 1:1.

2.3.2. Preparation of Hb/GNPs-Hap/GCE Modified Electrode

Glassy carbon electrode (GCE, 3 mm in diameter) was polished to a mirror-like with 1.0, 0.3 and 0.05 μm alumina slurry (Buehler) followed by rinsing thoroughly with doubly distilled water. The electrode was successively sonicated in 1:1 nitric acid, acetone and doubly distilled water for 2min, and then allowed to dry at room temperature. 10 μL of 5.0 mg mL^{-1} Hb solution and 5 μL of the obtained GNPs-Hap nanocomposite solution were finally cast on the GCE surface to obtain the Hb/GNPs-Hap/GCE.

As control, 5 μL of GNPs-Hap suspension was cast on GCE to obtain a GNPs-Hap/GCE; 10 μL of 5.0 mg mL^{-1} Hb solution and 5 μL water were cast on GCE to obtain a Hb/GCE; 10 μL of 5.0 mg mL^{-1} Hb solution and 5 μL Hap suspension were cast on GCE to obtain a Hb/Hap/GCE; and 10 μL of 5.0 mg mL^{-1} Hb solution and 5 μL GNPs solution were cast on GCE to obtain a Hb/GNPs/GCE.

After dropped these mixtures, a small bottle was fit tightly over the electrode for 2 h to ensure the slow evaporation of water and the formation of uniform film. The film was then dried and aged overnight in a sealed flask at room temperature. Prior to electrochemical experiments, the electrodes were rinsed thoroughly with doubly distilled water and kept in 0.1 M pH 7.0 PBS at 4 °C in a refrigerator when not use.

3. Results and Discussion

3.1. Optimization of GNPs-Hap Nanocomposite

The volume ratio of Hap suspension to GNPs solution was a key factor for obtaining a stable film of GNPs-Hap nanocomposite with high carrying capacity. High content of Hap nanotubes in the nanocomposite could increase the carrying capacity of both GNPs and protein. But the electric resistance of the resulting nanocomposite film also increased, which was disadvantageous to the direct electron transfer of the immobilized protein. Contrarily, at low content of Hap nanotubes the formed nanocomposite film was unstable. It could easily be brushed off. Moreover, the carrying capacity was also decreased. An appropriate volume of Hap suspension to GNPs solution with the maximum current response of the Hb/GNPs-Hap/GCE could be obtained to be 1:1, at which the formed film was also stable enough for electrochemical and biosensor study. Thus the volume ratio of 1:1 was used for the preparation of GNPs-Hap nanocomposite in whole experiment.

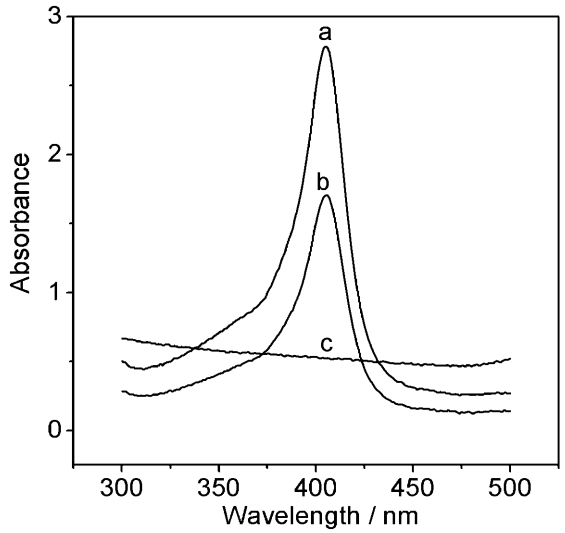

Fig. 1. UV-vis spectra of Hb/GNPs-Hap (a), Hb (b), GNPs-Hap (c) dispersed in water.

3.2. UV-Vis Spectroscopic and SEM Characterization

UV-vis spectroscopy is a useful conformational probe for heme proteins. The location of the Soret absorption band provides structural information about possible denaturation of heme proteins, especially conformational change in the heme group region [36]. It can be observed from Figure 1 that both films containing Hb displayed a maximum absorption at 405 nm (curve a, b), while no absorption of GNPs – Hap was observed (curve c). Obviously, the absorption peak was attributed to the Soret band of Hb. No shift of the Soret band upon mixing of Hb with GNPs-Hap was observable. Thus GNPs – Hap did not change the fundamental microenvironment of Hb. The Hb mixed in the nanocomposite film retained its natural secondary structure.

The morphology of the modified electrodes was also characterized by SEM. Figure 2 displays typical SEM images of Hap and GNPs – Hap nanocomposite films. The SEM image of Hap shows a nanotube structure, and Hap dispersed very well. In GNPs – Hap nanocomposite film GNPs can strongly adsorb on the surface of Hap to form a uniform porous structure, which increases the homogeneous loading of protein.

3.3. Direct Electrochemistry of Hb/GNPs-Hap/GCE

The cyclic voltammograms of Hb/GNPs-Hap/GCE displayed a couple of stable and well-defined redox peaks at -308 mV and -372 mV at 100 mV s^{-1}, while no obvious

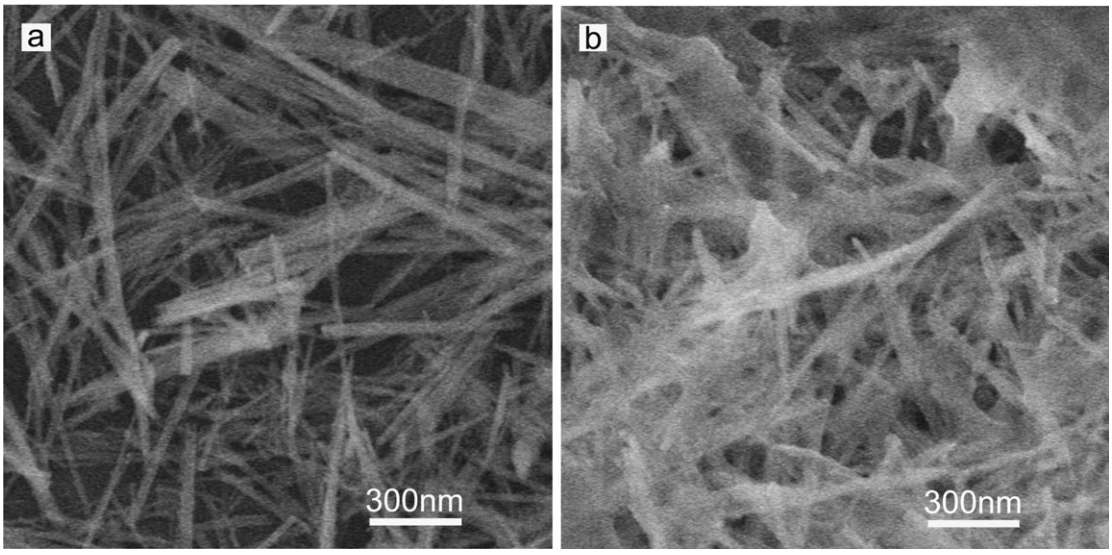

Fig. 2. Scanning electron micrographs of Hap (a) and GNPs-Hap (b) films.

electrochemical response was observed at both GCE and GNPs-Hap/GCE (Figure 3). Thus these peaks were attributed to the redox reaction of the electroactive center of Hb. However, Hb/GCE, Hb/Hap/GCE, Hb/GNPs/GCE exhibited only much smaller redox peaks of the electroactive center. The reduction peak currents at Hb/GNPs-Hap, Hb/Hap and Hb/GNPs modified electrodes were 3.6, 1.2 and 1.9 times larger than that at Hb/GCE, respectively. In spite of the same amount of Hb immobilized on electrode surface, the increase of peak current at Hb/GNPs-Hap modified electrode was not the sum of those at Hb/Hap and Hb/GNPs modified electrodes, indicating a synergic effect between GNPs and Hap for accelerating the surface electron transfer of Hb. The synergic effect came from the formation of GNPs-Hap nanocomposite. The nanocomposite showed good dispersion of GNP and some holes or channels (Figure 2b), which led to stronger ability of GNP to promote the electron transfer than those directly absorbed on GCE surface.

The formal potential $E_{1/2}$ of the $Fe^{III/II}$ couple in Hb/GNPs-Hap matrix, estimated as the midpoint of reduction and oxidation potentials, was about $-(340 \pm 2)$ mV (vs. SCE) in 0.1 M pH 7.0 PBS. This value was similar to those of -345 mV at Hb-meso-Al_2O_3 [37] and -340 mV at Hb/CMC-TiO_2-NTs [38], suggesting that most molecules preserved their native structure after being entrapped in the GNPs-Hap matrix. The cyclic voltammograms of the Hb/GNPs-Hap modified GCE in 0.1 M PBS solution at different scan rates were shown in Figure 4. With an increasing scan rate ranging from 10 to 1000 mV s^{-1}, the anodic and cathodic peak potentials of Hb showed a small shift and the peak-to-peak separation also increased, while the reduction and oxidation peak currents increased linearly (inset in Figure 4). These results indicated that the redox process was typical surface-controlled process. When the scan rate was returned to 100 mV s^{-1} from a higher scan rate, the shape of cyclic voltammogram and the peak positions were the same as the beginning those, with which Hb can be proved to adsorb firmly. According to $\Gamma = Q/nFA$, where Γ is the coverage of electroactive hemoglobin and Q represents the electric quantity consumed in the electrode process, the amount of electroactive hemoglobin molecules at the Hb/GNPs-HAP/GCE was estimated to be 9.54×10^{-13} mol cm^{-2}, which was much larger than those of 4.56×10^{-13} mol cm^{-2} at Hb-MCWC [39], indicating a better loading of the Hb in the nanocomposite matrix.

Figure 5 shows the effect of solution pH on direct electrochemistry of the immobilized Hb. With the increasing solution pH from 5.0 to 9.0, the negative shift of both reduction and oxidation peak potentials was observed. In general, all changes in the peak potentials and currents with solution pH were reversible in the pH range from 5.0 to 9.0. The plot of formal potential versus pH showed a slope of -51 mV pH^{-1} ($R = 0.993$) (inset in Figure 5a), which was close to the -59.2 mV pH^{-1} expected for a reversible, one-electron coupled one-proton reaction process at 25 °C. Thus one proton participated in the electrode reaction for neutralizing the excess charge that accumulated at the

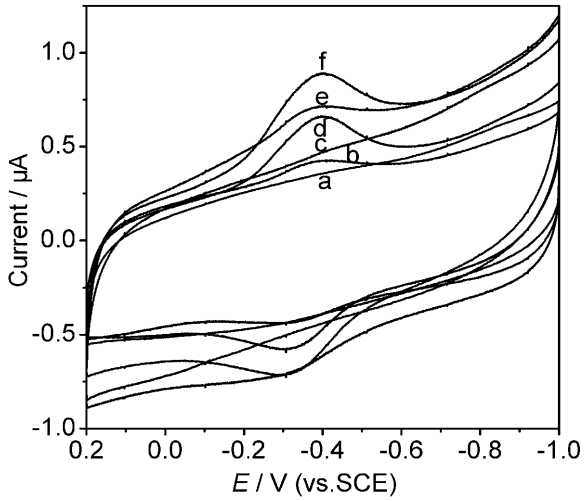

Fig. 3. Cyclic voltammograms of GCE (a), Hb/GCE (b), GNPs-Hap/GCE (c), Hb/GNPs/GCE (d), Hb/Hap/GCE (e), Hb/GNPs-Hap/GCE (f) in 0.1 M pH 7.0 PBS at 100 mV s^{-1}.

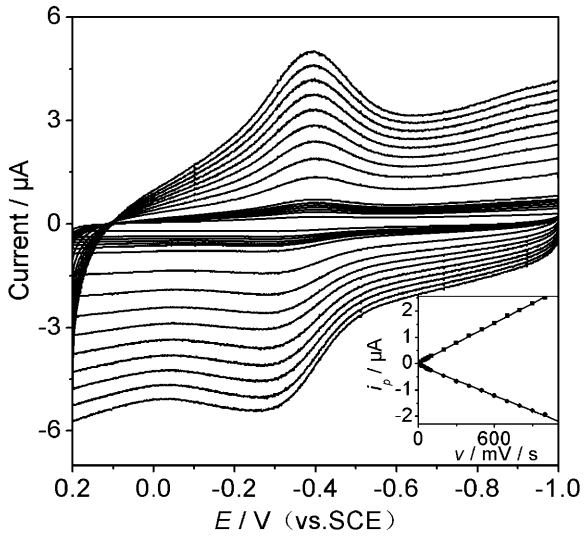

Fig. 4. Cyclic voltammograms of Hb/GNPs-Hap/GCE in 0.1 M pH 7.0 PBS at 10, 20, 30, 40, 50, 60, 70, 80, 90, 100, 200, 300, 400, 500, 600, 700, 800, 900, and 1000 mV s^{-1} (from lowest to highest peak current). Inset: plots of i_{pa} and i_{pc} vs. v

interface upon electrochemical reduction. The pH value also affected the peak currents of the direct electrochemistry. As shown in inset in Figure 5b the immobilized Hb showed the maximum peak current at pH 7.0, at which the heme-peroxidase generally shows maximum enzymatic activity.

3.4. Electrocatalysis of Hb/GNPs-Hap/GCE to Reduction of H_2O_2

It is well known that heme proteins can catalyze the reduction of H_2O_2. The electrocatalytic behavior of Hb/GNPs-Hap modified GCE was tested by amperometric

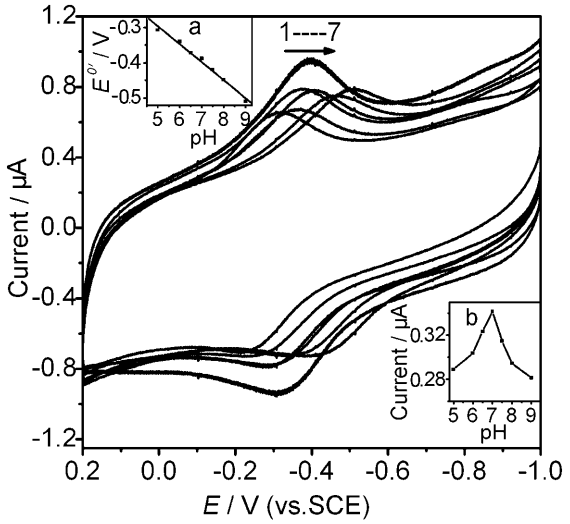

Fig. 5. Cyclic voltammograms of Hb/GNPs-Hap/GCE in 0.1 M pH 5.0, 6.0, 6.5, 7.0, 7.5, 8.0, and 9.0 (from 1 to 7) PBS at 100 mV s^{-1}. Inset: a) plot of formal potential vs. pH and b) effect on cathodic peak current.

measurements. Upon addition of H_2O_2 to 0.1 M pH 7.0 PBS, the cyclic voltammogram of Hb/GNPs-Hap/GCE for the direct electron transfer of Hb changed dramatically with an increase of reduction peak current and a decrease of oxidation peak current (Figure 6a), while the change of cyclic voltammogram of GNPs-Hap modified GCE was negligible (not shown), displaying an obvious electrocatalytic behavior of the Hb to the reduction of H_2O_2.

The electrocatalytic reduction peak of H_2O_2 by Hb/GNPs-Hap/GCE could be used to quantitatively determine the concentration of H_2O_2. Figure 6b shows the amperometric $i-t$ curve of the modified GCE with successive injection of H_2O_2 into pH 7.0 PBS at an applied potential of -372 mV, the reduction peak potential of Hb/GNPs-Hap/GCE at 100 mV s^{-1}. The biosensor showed very quick response, which could reach the stable current value in 15 second. The amperometric response increased linearly with the increase of hydrogen peroxide concentration in the range of 0.5–25 μM ($R=0.9990$, $n=19$) with a detection limit of 0.2 μM, which was lower than those of Hb-based biosensors for H_2O_2, as listed in Table 1. When H_2O_2 concentration was higher than 25 μM, a response plateau was observed, showing a typical Michaelis–Menten kinetic mechanism. The apparent Michaelis–Menten constant (K_M') could be calculated to be 3.64 μM from the Lineweaver–Burk equation [40]. The value of K_M' was smaller than those reported for Hb immobilized on the other electrode surfaces [41, 42]. The smaller K_M' meant that the present Hb exhibited higher affinity to H_2O_2.

Table 1. Detection limits of different Hb-based H_2O_2 biosensors. PDDA: poly(diallydimethylammonium); CIN: carbon-coated iron nanoparticles; CMC: carboxymethyl cellulose; NTs: nanotubes; UND: undoped nanocrystalline diamond.

Electrode	Detection limit	Reference
Hb/GNPs-Hap/GCE	0.2 μM	This work
{MSU/Hb}n/PDDA/GCE	0.5 μM	[9]
Hb/CIN-chitosan/GCE	1.2 μM	[10]
Hb-Au/GCE	5.5 μM	[28]
Hb/attapulgite/GCE	2.4 μM	[30]
Hb-Gel/GCE	3.4 μM	[31]
Hb/Chit/UND/GCE	0.4 μM	[32]
Hb/CMC-TiO_2-NTs/GCE	4.64 μM	[38]

3.5. Repeatability and Stability of Biosensor for Hydrogen Peroxide

The repeatability and stability of the biosensor was investigated by determining 20 μM H_2O_2 in 0.1 M PBS (pH 7.0). Five biosensors, made independently, showed a relative standard deviation (RSD) of 3.9% for current measurements. After the biosensor was kept at 4 °C for 30 days, it could retain 82.9% of its initial response. When it was used to consecutively measure the response of 0.1 mM H_2O_2 in 0.1 M pH 6.5 PBS, it lost 6.6% of the initial response after

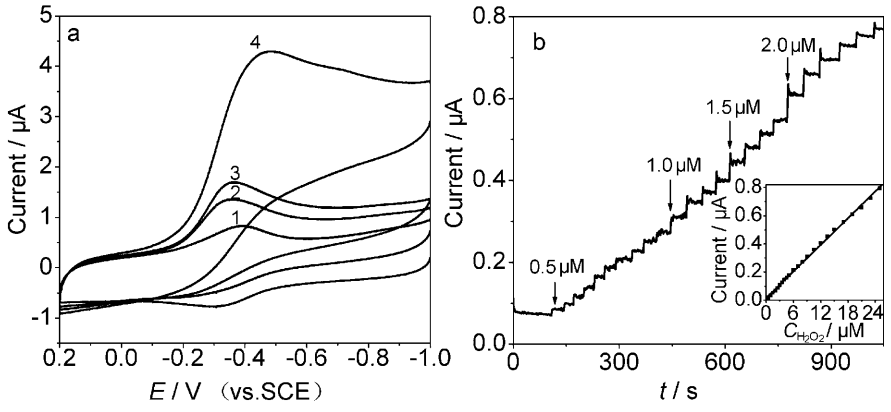

Fig. 6. a) Cyclic voltammograms of Hb/GNPs-Hap/GCE in 0.1 M pH 7.0 PBS containing 0 (1), 20 (2), 40 (3), and 200 μM (4) H_2O_2 at 100 mV s^{-1}. b) Typical current-time response curve of the biosensor upon successive additions of different amounts of H_2O_2 into 0.1 M pH 7.0 PBS at applied potential of -0.372 V. Inset in (b): plot of amperometric response vs. H_2O_2 concentration.

100 consecutive measurements. These results showed that the biosensor had good stability. The good stability of Hb-GNP-Hap/GCE was due to the presence of Hap with a hexahedron frame.

4. Conclusions

In this work, Hap nanotubes, a typical bone substitute material, has been used to prepare a new nanocomposite of GNPs-Hap, which is demonstrated as a biocompatible matrix for Hb immobilization. The resulting Hb/GNPs-Hap possessed good electron transfer properties for the protein with a synergic effect between GNPs and Hap for accelerating the surface electron transfer of Hb. The as-prepared Hb/GNPs-Hap/GCE displays high electrocatalytic performance toward reduction of H_2O_2 with fast response. The biosensor shows good stability and acceptable repeatability.

5. Acknowledgements

We gratefully acknowledge the support of the National Science Fund for Creative Research Groups (20521503), the Key Program (20535010), and Major Research Plan (90713015) from the National Natural Science Foundation of China and the Natural Science Foundation of Jiangsu Province (BK200814).

6. References

[1] F. A. Armstrong, G. S. Wilson, *Electrochim. Acta* **2000**, *45*, 2623.
[2] H. Y. Liu, N. F. Hu, *Anal. Chim. Acta* **2003**, *481*, 91.
[3] M. Pumera, S. Sánchez, I. Ichinose, J. Tang, *Sens. Actuators B* **2007**, *123*, 1195.
[4] C. X. Cai, J. Chen, *Anal. Biochem.* **2004**, *325*, 285.
[5] S. Q. Liu, D. Leech, H. X. Ju, *Anal. Lett.* **2003**, *36*, 1.
[6] Q. Zhang, L. Zhang, B. Liu, X. B. Lu, J. H. Li, *Biosens. Bioelectron.* **2007**, *23*, 695.
[7] C. H. Lie, U. Wollenberger, N. Bistolas, A. G. Elie, F. W. Scheller, *Anal. Bioanal. Chem.* **2002**, *372*, 235.
[8] C. Y. Liu, J. M. Hu, *Electroanalysis* **2008**, *20*, 1067.
[9] Z. Y. Sun, Y. Q. Li, T. S. Zhou, Y. Liu, G. Y. Shi, L. T. Jin, *Talanta* **2008**, *74*, 1692.
[10] H. L. Zhang, X. Z. Zou, G. S. Lia, D. Y. Han, F. Wang, *Electroanalysis* **2007**, *19*, 1869.
[11] D. Mimica, J. H. Zagal, F. Bedioui, *J. Electroanal. Chem.* **2001**, *497*, 106.
[12] J. W. Li, L. H. Liu, R. Yan, M. Y. Xiao, L. Q. Liu, F. Q. Zhao, B. Z. Zeng, *Electrochim. Acta* **2008**, *53*, 4591.
[13] X. J. Liu, T. Chen, L. F. Liu, G. X. Li, *Sens. Acuators B* **2006**, *113*, 106.
[14] J. Yang, N. F. Hu, *Bioelectrochem. Bioenerg.* **1999**, *48*, 117.
[15] L. Zhang, X. Jiang, E. Wang, S. J. Dong, *Biosens. Bioelectron.* **2005**, *21*, 337.
[16] G. Zhao, J. J. Feng, J. J. Xu, H. Y. Chen, *Electrochem. Commun.* **2005**, *7*, 724.
[17] S. Morita, K. Furuya, K. Ishihara, N. Nakabayashi, *Biomaterials* **1998**, *19*, 1601.
[18] B. J. Melde, A. Stein, *Chem. Mater.* **2002**, *14*, 3326.
[19] H. Zejli, K. Temsamani, P. Sharrock, *Chemospere* **2005**, *60*, 1157.
[20] C. A. Daykin, O. Corcoran, S. H. Hansen, I. Bjornsdottir, C. Cornett, S. C. Connor, J. C. Lindon, J. K. Nicholson, *Anal. Chem.* **2001**, *73*, 1084.
[21] R. M. Chicz, F. E. Regnier, *Anal. Chem.* **1989**, *61*, 1742.
[22] L. Yang, W. Z. Wei, X. H. Gao, J. J. Xia, H. Tao, *Talanta* **2005**, *68*, 40.
[23] Y. J. Ding, J. Liu, H. Wang, G. Shen, R. Q. Yu, *Biomaterials* **2007**, *28*, 2147.
[24] J. S. Xu, G. C. Zhao, *Electroanalysis* **2008**, *20*, 1200.
[25] S. Q. Liu, H. X. Ju, *Anal. Biochem.* **2002**, *307*, 110.
[26] Y. L. Yao, K. K. Shiu, *Electroanalysis* **2008**, *20*, 1542.
[27] S. Q. Liu, H. X. Ju, *Analyst* **2003**, *128*, 1420.
[28] X. X. Xu, S. Q. Liu, H. X. Ju, *IEEE Sens. J.* **2004**, *4*, 390.
[29] S. Q. Liu, H. X. Ju, *Anal. Biochem.* **2002**, *307*, 110.
[30] H. Yao, N. Li, J. Z. Xu, J. J. Zhu, *Talanta* **2007**, *71*, 550.
[31] J. T. Zhou, C. G. Shi, J. J. Xu, H. Y. Chen, *Bioelectrochemistry* **2007**, *71*, 243.
[32] S. Z. Zong, Y. Cao, H. X. Ju, *Electroanalysis* **2007**, *19*, 841.
[33] S. Z. Zong, Y. Cao, Y. M. Zhou, H. X. Ju, *Anal. Chem. Acta* **2007**, *582*, 361.
[34] H. J. Lee, H. W. Choi, K. J. Kim, S. C. Lee, *Chem. Mater.* **2006**, *18*, 5111.
[35] K. R. Brown, A. P. Fox, M. J. Natan, *J. Am. Chem. Soc.* **1996**, *118*, 1154.
[36] X. B. Lu, J. Q. Hu, X. Yao, Z. P. Wang, J. H. Li, *Biomacromolecules* **2006**, *7*, 975.
[37] J. J. Yu, J. R. Ma, F. Q. Zhao, B. Z. Zeng, *Electrochim. Acta* **2007**, *53*, 1995.
[38] W. Zheng, Y. F. Zheng, K. W. Jin, N. Wang, *Talanta* **2008**, *74*, 1414.
[39] G. X. Ma, Y. G. Wang, C. X. Wang, T. H. Lu, Y. Y. Xia, *Electrochim. Acta* **2008**, *53*, 4748.
[40] R. A. Kamin, G. S. Willson, *Anal. Chem.* **1980**, *52*, 1198.
[41] M. R. Li, C. Y. Deng, C. Chen, L. M. Peng, G. H. Ning, Q. J. Xie, S. Z. Yao, *Electroanalysis* **2006**, *18*, 2210.
[42] J. J. Feng, G. Zhao, J. J. Xu, H. Y. Chen, *Anal. Biochem.* **2005**, *342*, 280.

